Limnol. Oceanogr., 30(6), 1985, 1171–1187

Wave forces on intertidal organisms: A case study[1]

Mark W. Denny[2]
Department of Zoology, University of Washington, Seattle 98195, and
Biological Sciences Department, Stanford University, Hopkins Marine Station,
Pacific Grove, California 93950

Abstract

Breaking waves impose large forces on intertidal organisms, and these forces are important in structuring wave-swept communities. Here a telemetry system is used to continuously record wave forces at an exposed site; the interpretation of one such record is presented as a case study of the nature of wave forces. For waves with a breaking height of 2–4 m, water velocities of at least 8 m s^{-1} and accelerations of at least 400 m s^{-2} are present near the substratum. The forces imposed on organisms by these flows depend on the size and shape of the organism. For a limpet (*Collisella pelta*) an average force is about 0.6 N, a maximum about 3 N. The magnitude and direction of wave forces are unpredictable in both time and space over periods of seconds to hours, although predictability is possible over longer periods. A quantitative exposure index, based on an organism's ability to withstand wave forces, shows that various organisms exposed to the same flow are at widely varying risks. No impact forces were observed during this study.

Breaking waves subject intertidal organisms to large hydrodynamic forces (Denny 1982, 1983; Denny et al. 1985), and these forces play an important role in many aspects of intertidal existence. For example, filter- and suspension-feeding animals rely on waves to circulate water past them but must also cope with the forces imposed by flow (Koehl 1977, 1982, 1984). When wave forces are too severe, mobile predators (e.g. starfish and thaid snails) and herbivores (e.g. littorine snails and limpets) may be unable to forage (Menge 1972, 1978; Lubchenco and Menge 1978; Wright 1978; Quinn 1979). Wave forces can break or dislodge organisms, in the process opening patches of substratum for settlement or invasion (e.g. Connell 1972; Paine and Levin 1981; Denny et al. 1985). Disturbances caused in this manner may control various aspects of intertidal communities (e.g. Quinn 1979; Paine and Levin 1981; Sousa 1984). In fact, it has been standard practice for many years to correlate the assemblage of organisms present on a shore with the "exposure" (Jones and Demetropoulos 1968; Ricketts et al. 1968; Lewis 1968; Newell 1979). The term exposure has generally been taken to be some integrated index of the severity of the wave action. An exposed site is subjected to frequent, large wave forces, and it is assumed that these forces cause frequent disturbance to the communities present. A protected site, in contrast, is subjected less frequently to forceful wave action, with a concomitant decrease in wave-caused disturbance.

As important as the wave-force environment is in determining intertidal community structure, actual measurements of wave forces (and, therefore, of exposure) have been rare. Harger (1970) measured cumulative wave force using a small plate attached to a nail by a friction fitting and correlated these measurements with several aspects of the biology of mussels, with some success in predicting adhesive tenacity, size, and growth rate. However, the cumulative nature of Harger's measurements makes them a less-than-adequate measure of exposure because many small forces yield the same index of exposure as do a few large forces. However the action of many small forces, each presenting no physical danger to an organism, may have entirely different biological consequences from a few large forces capable of breaking or dislodging the organism. The converse problem is inherent in the method of force measurement used by Jones and Demetropoulos (1968). A recording spring scale was attached to a small disk and used to record the maximum force

[1] This study was supported by ONR contract N00014-79-C-0611 with logistic support from NSF grant OCE 77-26901 to R. T. Paine.
[2] Present address: Hopkins Marine Station, Pacific Grove, California 93950.

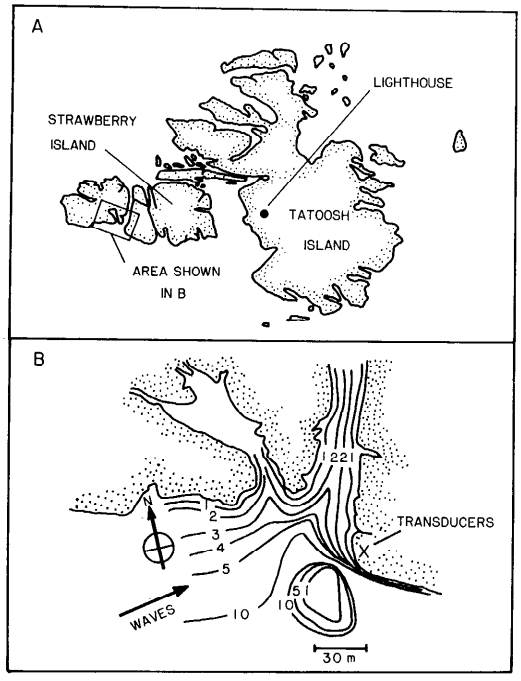

Fig. 1. A. Tatoosh Island. B. The study site on Strawberry Island. Lines of equal depth are in meters.

encountered over a series of tides. This technique provides no information regarding the number of forces encountered or the direction of their application. Both methods have the disadvantage of measuring the force on a thin, flat plate rather than that actually exerted on an organism. The turbulent nature of flow in the surf zone makes it difficult to interpret the results of these studies in terms either of the water velocity and acceleration which caused them or of the force imposed on a particular organism. There are also problems having to do with the long response time of these apparatus (*see* Denny 1982, 1983).

Two apparatus have been constructed to circumvent these problems. Koehl (1977) used a force platform situated in a surge channel to record the time-averaged forces imposed on the anemone *Anthopleura xanthogrammica*. Although this apparatus can measure the force actually exerted on an organism, it does so only by measuring the average difference between forces on the platform with and without the organism present. Thus, the force due to a single wave cannot be measured. The response time of the apparatus is also likely to be too long to record transiently applied forces. Denny (1982) designed a telemetry system that can measure the components of force exerted by individual waves on organisms. The response time of this apparatus (about 8 ms) is sufficient to accurately record all but the most rapidly applied forces, and this temporal accuracy allows calculation of the flow velocities and accelerations causing wave forces. Using this apparatus, I continuously recorded individual wave forces through entire tidal cycles at an exposed site on the Pacific coast of Washington. The interpretation of one representative set of these records is presented here as a case study of the nature of wave forces.

I thank R. T. Paine and the U.S. Coast Guard for the opportunity to conduct this research on Tatoosh Island. D. Ferrell, R. Reinstatler, F. Ward, and S. Palumbi provided technical support. The manuscript profited from the comments of S. Gaines, C. Baxter, D. Lindberg, and an anonymous reviewer. S. Denny and K. Denny provided moral support.

Methods

Site—This study was conducted on Tatoosh Island, off the tip of the Olympic Peninsula (124°44′W, 48°23′N). The force transducers were emplaced on the southwest point of one of the subislands of Tatoosh (Strawberry Island: Fig. 1) on a roughly planar section of rock inclined about 35° from the horizontal.

The seafloor slopes irregularly down from this site (Fig. 1), with depths of 10 m (below MLLW) within about 30 m. Waves impinging on the site are generally of the types termed "collapsing" or "surging" (Galvin 1972); I have never observed a typical "plunging" breaker there. The site is fully exposed to the prevailing southwesterly swells.

Holes for the emplacement of the telemetry system force transducers were chiseled into the rock about 3.5 m above MLLW, in the middle of the *Balanus glandula* zone (zone 1: Ricketts et al. 1968). Similar emplacements at the same site held maximum wave-force recorders at heights of 2.75 m

(just above the upper limit of a bed of *Mytilus californianus*) and at 1.65 m (in the lower reaches of the mussel bed).

Telemetry system—The wave-force telemetry system (Denny 1982) was used for all measurements of individual wave forces. Three force transducers were installed in a triangular array with their upper surfaces flush with the rock substratum. The distance between transducers was 10–15 cm. Each transducer measured force in one direction; the two measuring forces in the plane of the substratum (shear forces) were oriented so that they measured force in either a shoreward–seaward direction or across the rock face (left–right as viewed from the sea), the third measured forces directed normal to the plane of the substratum (into or out of the rock). The voltage signal from each transducer was conducted by cable to the telemetry system above the surf zone and the signals were converted to frequency-modulated audio signals, combined, and transmitted as a radio signal to a receiver in the lighthouse on Tatoosh Island. The audio signal was tape recorded and the records returned to the lab for transcription onto an oscillographic chart recorder. The telemetry system was calibrated in the laboratory (transducers at 8.5°C) immediately before we left for Tatoosh.

Measurements were made with identical objects mounted on all three transducers. I used three types of objects: cast epoxy replicas of a limpet (*Collisella pelta*) and an acorn barnacle (*Semibalanus cariosus*), and small (1.9-cm diameter) acrylic spheres. The primary results considered here were for the limpet replicas ($C_D = 0.45$ at Reynolds number 10^5: Denny et al. 1985; $C_M = 1.68$: Denny et al. 1985; terms defined in Eq. 1, 2 below). The replicas were oriented on the shear-force transducers with the anterior-posterior axis of the shell parallel to the direction of the force being measured. Their base-to-peak height is 1.1 cm, so that the forces measured are due to flows very near the substratum. Denny et al. (1985) proposed that the boundary layer (a layer of fluid near the substratum with a retarded velocity) is maximally 0.5 cm; it is probably smaller in the types of flows encountered here (*see also* Nowell and Jumars 1984).

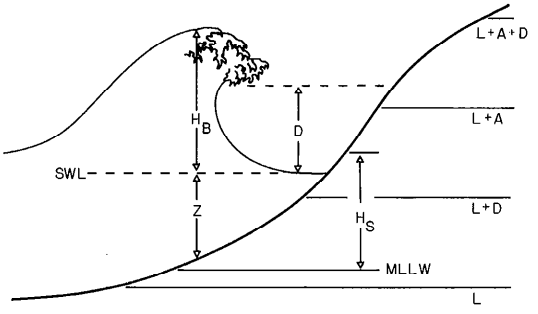

Fig. 2. A schematic representation of a breaking wave defining various terms. H_B—Wave height at breaking; Z—water depth under a breaking wave; SWL—still-water sea level; D—the vertical height of the main body of the wave; MLLW—mean lower low water (chart datum for U.S. maps); H_S—height of an organism on the shore; L—low tide level (shown here for a minus tide); A—amplitude of the tidal excursion. The wave shown here is a plunging breaker, but the same terms can be applied to surging and collapsing breakers.

Thus the forces imposed on the limpet replicas are probably caused by essentially mainstream flows.

Choice of sample record—During this study (18 tidal cycles, about 100 h of data recorded) low tides appropriate for the installation of the telemetry system did not coincide with any major storms, so that the wave forces recorded are not the maximum likely to occur at this site. The records from the roughest day (evening, 19–20 November 1980) are used as the primary data base. Waves visually estimated to have peak-to-trough heights at breaking (H_B, Fig. 2) of 2–4 m were common during this period, comprised of both sea and swell. The presence of short-period, locally produced seas resulted in an average wave period of 6–8 s, somewhat below that typical of Pacific swell (10–14 s: U.S. Army Corps of Eng. 1977). The wave direction was generally from the southwest, and waves broke directly on the study site.

Direction and magnitude of maximum force—In addition to the measurements made with the telemetry system, I made a series of measurements with a device capable of recording the direction and magnitude of the maximum wave force encountered during a high tide (Denny 1983). Small spheres (1.9-cm diameter) were

mounted on three recorders installed at each of three heights (1.65, 2.75, and 3.50 m above MLLW) on seven tides during June, July, August, and September 1980. Additional measurements were made at the mid-level emplacement throughout the study. The average direction and radial distribution of directions were calculated as suggested by Zar (1974).

Interpretation of results—The data gathered here concern the *force* exerted on a replica limpet and other shapes. The usefulness of these data can be extended by viewing the forces in terms of the *flow* which caused them. A brief discussion of the nature of flow-induced forces is thus in order.

At the high Reynolds number values encountered in the wave-swept environment (typically 10^4–10^6: *see* Vogel 1981 for a discussion of the Reynolds number), the forces exerted on nonstreamlined objects are primarily of three sorts.

First, drag. The flow pattern around an object results in a difference in pressure between the upstream and downstream sides of the object, with the pressure higher upstream. The pressure difference is proportional to the dynamic pressure of the moving fluid ($0.5\rho U^2$) where ρ is the density of seawater (about 1,025 kg m^{-3}) and U is the water velocity. The force caused by the pressure difference is equal to the pressure difference times the area over which it acts. In this case the area is that projected in the direction of flow, S (Vogel 1981). The pressure drag is thus proportional to $0.5\rho U^2 S$. In addition to the drag caused by a pressure difference, there is a drag (friction drag) due directly to the sliding of a viscous fluid (e.g. seawater) past the object. The combination of pressure and friction drags can be related to the dynamic pressure through the inclusion of an appropriate coefficient of proportionality, the drag coefficient, C_D:

$$\text{Drag} = 0.5\rho U^2 S C_D. \tag{1}$$

Drag acts in the direction of flow.

Second, the acceleration reaction. If the flow past an object changes velocity through time, the object experiences a force proportional to the water's acceleration. Unlike pressure drag, which is proportional to projected area, this acceleration reaction is proportional to the volume of water displaced by the object, V:

$$\text{Acceleration reaction} = \rho V(\mathrm{d}U/\mathrm{d}t)C_M \tag{2}$$

where C_M is a coefficient of proportionality determined largely by the shape of the object. For stationary objects such as those examined here, $C_M = 1 + C_A$, where C_A is the added mass coefficient (Batchelor 1967; Sarpkaya and Isaacson 1981; Daniel 1982, 1984). The acceleration reaction acts along the direction of flow and, depending on whether the flow is accelerating or decelerating, may add to or subtract from the pressure drag.

To a first approximation, the total force in the direction of flow is the sum of the pressure drag and the acceleration reaction (Sarpkaya and Isaacson 1981):

$$\text{Force in direction of flow} = 0.5\rho U^2 S C_D + \rho V(\mathrm{d}U/\mathrm{d}t)C_M. \tag{3}$$

Third, lift. If the morphology of the object is such that a layer of water (or any other material capable of transmitting hydrostatic pressure, i.e. guts) is present between the object and the substratum, the flow pattern may be such that the object experiences a force perpendicular to the direction of flow—a lift. As with pressure drag, lift is caused by a pressure difference across the object, and the equation describing lift is therefore similar to that for drag:

$$\text{Lift} = 0.5\rho U^2 S_B C_L \tag{4}$$

where S_B is the area of the object projected in the direction of the lift. For most organisms (e.g. limpets) lift will be perpendicular to the substratum, and S_B is thus the basal area. C_L is the coefficient of lift.

The overall magnitude of force due to the combined action of pressure drag, acceleration reaction, and lift is obtained from the vector sum of the individual forces. The direction of the overall force lies at an angle, θ, to the direction of flow, and in the plane determined by the lift and drag vectors. θ is the arctangent of the lift divided by the force in the direction of flow. Much more thorough discussions of flow-induced forces are

given by Batchelor (1967), Sarpkaya and Isaacson (1981), or Vogel (1981).

The records of individual wave forces were analyzed as follows.

Velocity and acceleration—The tape records for 30 sequential large waves were transcribed with the chart recorder at a chart speed of 100 mm s^{-1}. Chart recordings for shear forces were then enlarged and traced. The enlarged force: time tracings were digitized (points taken approximately every 2 ms) and the data entered into a computer. From these force: time data for the shear component of force, the components of velocity and acceleration causing the force were calculated by numerically solving Eq. 3 (Denny et al. 1985).

Because the force transducers are separated by about 10–15 cm, they do not sample identical volumes of fluid and therefore may be measuring different flows. It is thus not strictly appropriate to combine records from the three transducers to calculate an overall force vector for each individual wave: overall velocity and acceleration vectors cannot be calculated except as an average over many waves. The records from the three directional transducers are therefore analyzed separately.

Distribution of wave forces—The maximum force exerted by each wave was measured from the chart recordings to the nearest 0.035 N. Results were tabulated for all discernible wave forces (force > about 0.035 N) through the 6-h course of the tide.

Time between wave forces—In addition to measuring the magnitude of each wave force, I noted the time of the maximum force associated with each wave to the nearest second and tabulated the distribution of times between maximum forces and the variation in this interwave time as a function of wave force. In addition, the series of times-of-wave-force were used to calculate the power spectrum for maximum wave-force occurrences, which provides a measure of the predictability (in both time and magnitude) of the maximum forces caused by waves. Because the tape recordings from the telemetry system were maximally 90 min long, the time series for the 6-h surrounding high tide is divided into four segments, with gaps of about a minute between segments. The spectrum of each 90-min time series was calculated by the Blackman-Tukey procedure with a Bartlett window (Jenkins and Watts 1968). The overall spectrum was obtained by averaging the four individual spectra.

Correlation with tidal height—The record of wave forces was divided into 10-min segments ($n = 36$ for up-down data, $n = 38$ for shear-force data) with the time of high tide as zero time and the number and magnitude of wave forces noted for each segment. The frequency of occurrence of events of different forcefulness was calculated, i.e. the number of forces >0.2 N per 10-min segment, the number of forces >0.5 N per 10-min segment, etc. These frequencies were then correlated with both time from high tide and the calculated height of the still-water sea level (SWL). SWL was calculated assuming that tidal height varies so that the height at time t is

$$H(t) = 0.5A\{[\cos(\pi t/\tau)] + 1\} + L \quad (5)$$

where A is the amplitude of the tidal excursion (i.e. the height difference between low and high tide), τ is the time between high and low tides (usually about 6.15 h), and L is the water level at low tide (Fig. 2). Time t is measured in hours from high tide.

Results

Forces—The maximum and mean forces exerted on the replica *C. pelta* are given in Table 1. Both the mean and maximum normal forces are directed away from the substratum. From these data a mean vector force can be calculated: 0.63 N directed 239.9° counterclockwise from seaward (i.e. toward the shore and to the left as viewed from the sea) and at an angle, θ, of 43.3° away from the substratum. No two of the directional maximum forces occurred on the same wave. However, had all these forces occurred simultaneously, the net force on the limpet would be 4.68 N, directed 239.2° counterclockwise from seaward and at an angle of 45.9° to the surface of the substratum. This hypothetical force vector can be viewed as an estimate of the maximum force which could be associated with waves like those during the sample tide.

Velocity and acceleration—Figure 3 shows

Table 1. Mean and maximum values for force components recorded 19–20 November 1980.

Direction	Mean force (N)	*n*	Max force (N)
Shoreward–seaward	0.27 shoreward	955	1.67 shoreward
Left–right	0.37 left	996	2.80 left
Up–down	0.43 up	873	3.36 up

Mean force vector
Magnitude: 0.63 N
Angle in plane of substratum: 233.9° counterclockwise of seaward
Angle to plane of substratum: 43.3° up

Hypothetical maximum force vector
Magnitude: 4.68 N
Angle in plane of substratum: 239.2° counterclockwise of seaward
Angle to plane of substratum: 45.9° up

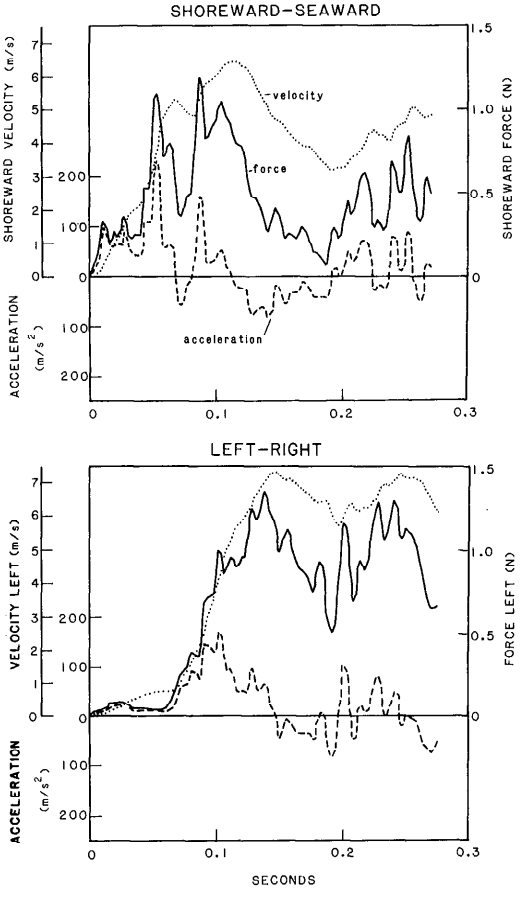

Fig. 3. Force, velocity, and acceleration components for the initial 0.3 s of a typical wave-force event. Velocity and acceleration were calculated from the recorded force as described in the text.

typical results for the calculation of the velocity and acceleration components causing the observed forces. The highest velocity component calculated for the 30 forceful waves examined was about 8 m s^{-1}. For the wave shown in Fig. 3, velocity components of 4.7 m s^{-1} shoreward and 7.3 m s^{-1} left occurred at the same time after the initial application of force. Assuming for the moment that these two transducers were sampling approximately the same flow, this is equivalent to an overall flow velocity of 8.7 m s^{-1}. Carstens (1968) and Galvin (1972) show that the maximum velocity, U_{max}, associated with a breaking wave occurs at the crest:

$$U_{max} = [g(H_B + Z)]^{1/2} \quad (6)$$

where g is the acceleration due to gravity (9.81 m s^{-1}), H_B is the trough–crest height of the breaking wave, and Z is the depth of the water under the breaking wave (Fig. 2). Waves break when the water depth is about 1.2 times the wave height (Galvin 1972). Thus:

$$U_{max} = [g(2.2H_B)]^{1/2}. \quad (7)$$

When H_B = 4 m (in accordance with visual observation), the maximum water velocity calculated from Eq. 6 is 9.3 m s^{-1}. Carstens (1968) suggests that on steeply sloping shores where waves break near the shore this crest velocity is likely to be the maximum velocity encountered by an organism at the substratum, and indeed this value compares well with the rough estimate for overall velocity calculated above from the force record (8.7 m s^{-1}).

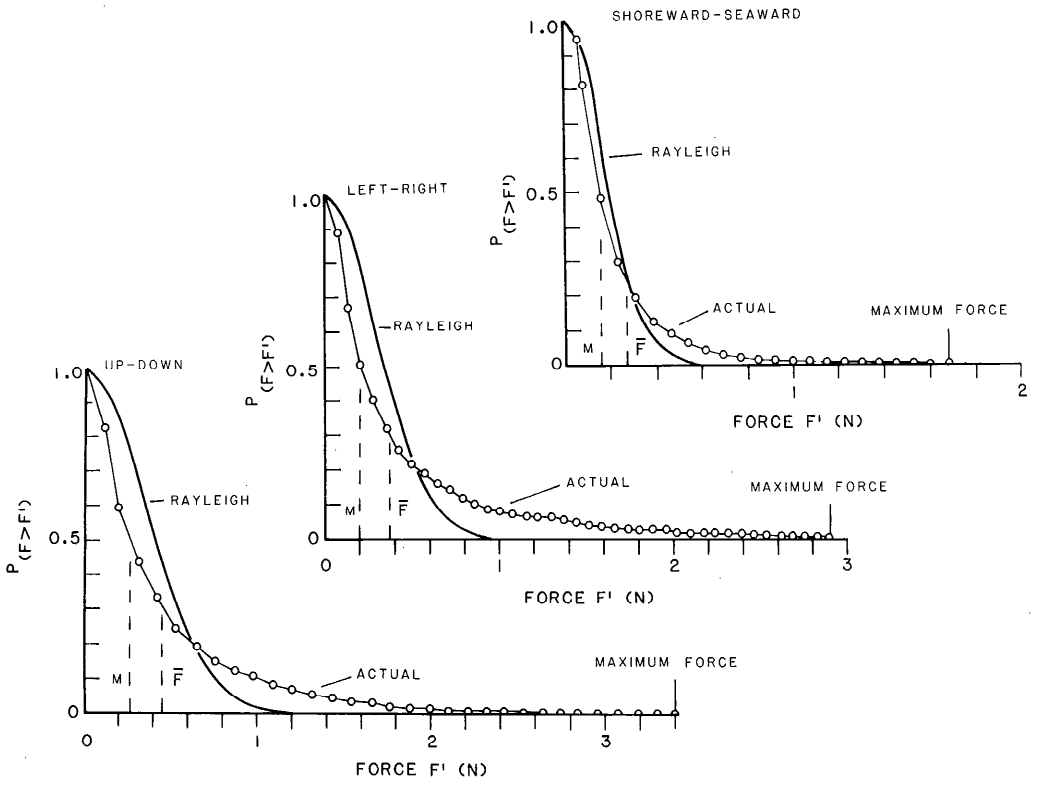

Fig. 4. Exceedance distributions for the three directions of wave force. $P_{(F>F')}$ is the probability that a wave, chosen at random, will cause a force, F, greater than F'. Rayleigh distributions are calculated for the observed mean forces. $\bar{F}$—Mean force; M—median force.

The maximum acceleration calculated from the force record was about 400 m s^{-2}. This may actually be an underestimate. Changes in force over periods <8 ms are not accurately recorded by the force transducers used, so that the recorded force is less than the actual force. This smoothing of peak forces could substantially decrease the acceleration calculated below that actually occurring. However, due to the very short duration of these unmeasured rapid accelerations (Fig. 3), their effect on the velocity would not be great.

Distribution of wave forces—The distribution of wave forces was tabulated for each force direction. From these tabulations the probability, $P_{(F>F')}$, was calculated that the force, F, exerted by a wave chosen at random would exceed a given level, F'. These exceedance distributions are shown in Fig. 4.

In each direction, the mean force is greater than the median force. This property is similar to that of a Rayleigh distribution, a theoretical distribution which accurately describes the distribution of offshore wave heights (Longuet-Higgins 1952; U.S. Army Corps of Eng. 1977), as well as the height of turbulent bores in the surf zone (Thornton and Guza 1983). This similarity deserves closer examination. As shown in Eq. 7, wave height at breaking is proportional to the square of velocity. Further, the square of velocity determines the drag and lift forces (Eq. 1 and 4). It thus might be supposed that offshore waves with a Rayleigh distribution of heights should, when breaking, cause drag and lift forces with a similar distribution. Following this reasoning, I calculated a Rayleigh distribution for each directional force mean. $P_{(F>F')}$ is given by

$$P_{(F>F')} = \exp[-(\pi/4)(F'/\bar{F})^2] \qquad (8)$$

where $\bar{F}$ is the mean force (Sarpkaya and Isaacson 1981). These calculated Rayleigh

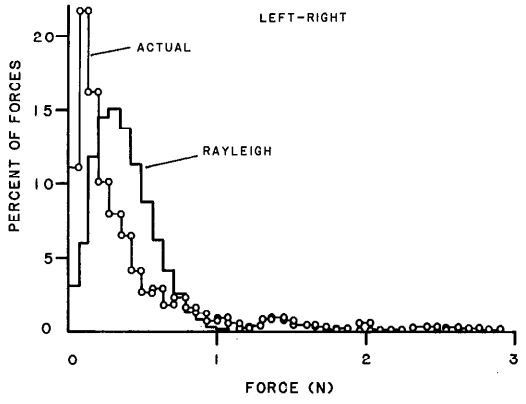

Fig. 5. The distribution of percent of wave forces as a function of force. Data are for the left–right force direction; other force directions have very similarly shaped distributions.

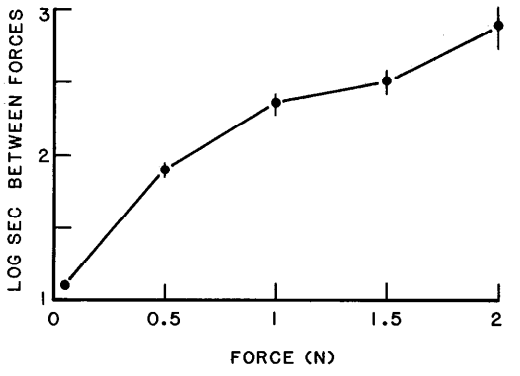

Fig. 7. Time between force events as a function of the minimum force of the events considered (data for the left–right component of force, 19–20 November 1980, means and standard errors shown).

exceedance distributions are shown in Fig. 4. In each case the observed distribution differs substantially and systematically from a Rayleigh distribution. There are fewer midrange forces in the observed record than predicted and more small and large forces. This can be seen more clearly when the distribution of forces rather than the probability of exceedance is plotted (Fig. 5). This deviation from a Rayleigh distribution could be due to either of two factors. The distribution of offshore wave heights was not measured and therefore could have a non-Rayleigh distribution. Alternatively, nonlinear effects near the breaking point could have affected the height distribution of waves (Thornton and Guza 1983), leading to non-Rayleigh distributions of forces. The present data are not sufficient to distinguish between these two possibilities.

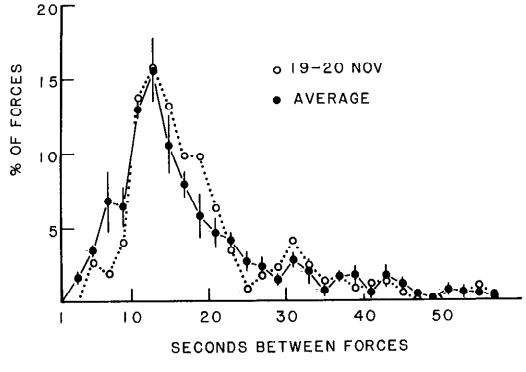

Fig. 6. Distribution of times between wave forces for 19–20 November 1980 (the sample record discussed here) and for this record averaged with three other records taken in April and May 1980 (means and standard errors shown).

Distribution of interwave interval—The distribution of times between maximum forces for the sample tide is shown in Fig. 6. The peak at 12–14 s is roughly twice the period of the incoming waves (about 6–8 s for the sample record), perhaps indicating that the backwash from one wave interferes with the subsequent wave. Similar patterns have been noted for waves breaking on sandy beaches (e.g. Guza and Bowen 1976; Guza and Thornton 1982). The interwave time distribution for this sample tide is very close to that from other tides; an averaged distribution from four tides is also shown in Fig. 6. These distributions do not take into account the force of waves; they are based solely on the interval between waves.

As expected, due to the decrease in the frequency of waves as the force of the wave increases (Fig. 5), the time between force events increases as the magnitude of the event considered increases; one example is shown in Fig. 7.

Power spectrum—The power spectrum of maximum wave forces is shown in Fig. 8. Each point represents an estimate of the variance of force at a certain frequency, calculated as the Fourier cosine transform of the autocovariance of the time series. Each spectral estimate has been divided by the

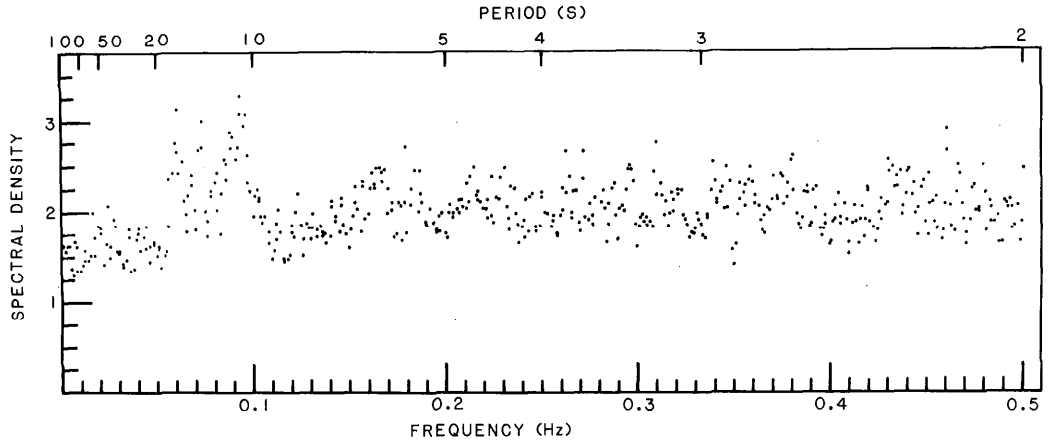

Fig. 8. Power spectrum for the time series of time-of-occurrence and maximum force from the record of the left–right component of force, 19–20 November 1980.

overall sample variance to give values of power spectral density. The area under any portion of the curve represents the contribution to the total variance of force events occurring with a certain range of frequencies. The spectrum is essentially flat, indicating that no frequency is any more probable than any other. The only discernible peaks are at frequencies around 0.09 Hz, i.e. at periods of 11–12 s, corresponding roughly to the peak in interwave time seen in Fig. 6. The spectrum was measured to frequencies as low as 0.001 Hz (periods of 1,000 s) and no low-frequency (long-period) peaks are evident. The occurrence of wave forces appears to be unpredictable over the time periods considered in this analysis for the combination of sea and swell present.

Frequency of force events correlated with water level and time—There is a significant correlation ($P < 0.05$) between the frequency of force events and the still-water level of the ocean when all force events are taken into account (Fig. 9, solid lines). However, as the magnitude of the force event taken into account increases, the strength of the correlation decreases. For the shoreward–seaward and up–down directions there is no significant correlation ($P > 0.05$) between still-water sea level and frequency of force impositions at the highest force level considered. In all cases there is no correlation at the 0.01 level at the highest forces considered. These correlations were calculated for the number of force events per 10-min segment vs. SWL; even though the number decreases as the magnitude of force considered increases, the number of 10-min seg-

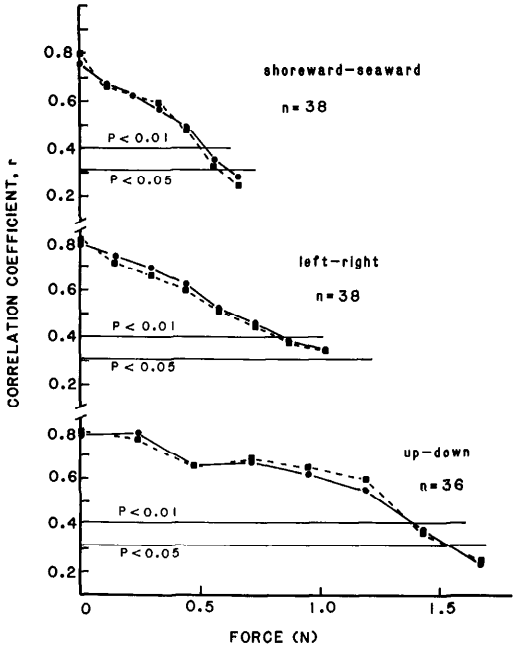

Fig. 9. Correlation of number of forces per 10-min period with either still-water sea level (solid lines) or time from high tide (dashed lines). As the minimum value of the forces considered increases, the correlation coefficient, r, decreases. The values above which r is significant are shown for two levels of significance ($P < 0.01$ and $P < 0.05$).

Table 2. Maximum and mean force components and their correlation with still-water sea level (SWL) and time from high tide. (N.S.—No significant correlation.)

Direction	n	Versus SWL			Versus time		
		r	r^2	P	r	r^2	P
Maximum force in each 10-min period							
Left–right	38	0.514	0.264	<0.001	0.474	0.255	<0.005
Shoreward–seaward	38	0.300	0.090	N.S.	0.069	0.005	N.S.
Up–down	36	0.412	0.170	<0.02	0.393	0.155	<0.02
Average force in each 10-min period							
Left–right	38	0.383	0.146	<0.02	0.333	0.111	<0.05
Shoreward–seaward	38	0.377	0.142	<0.05	0.362	0.131	<0.05
Up–down	36	0.581	0.337	<0.001	0.613	0.376	<0.001

ments stays constant (n = 36 or 38). Even for the largest forces considered there were at least five events per 10-min period in one or more of the periods.

Results were essentially identical when frequencies were correlated with time from high tide rather than SWL (Fig. 9, dotted lines).

Magnitude of force events correlated with water level and time—There are significant correlations ($P < 0.02$) between the maximum force recorded in each 10-min period and the still-water sea level for forces in both the left–right and up–down directions (Table 2). Although statistically significant, these correlations are far from striking (Fig. 10), accounting for at most 26% of the observed variation in maximum force (r^2, Table 2). There is no correlation between maximum force and water level in the shoreward–seaward direction.

Similar results are obtained when the maximum force in each 10-min period is correlated with time from high tide (Table 2).

For all force directions there is a significant correlation ($P < 0.05$) between the average force in each 10-min period and both still-water sea level and time from high tide (Table 2). Again, although these correlations are significant, they are not striking (Fig. 11), accounting for at most 38% of the variance in average force and more typically 10–15% (r^2, Table 2).

Maximum force as a function of height on shore—The results from the maximum force recorders placed at different heights on the shore are given in Table 3. The site at 2.75 m above MLLW had the highest average maximum force over the course of the seven tides, but the variance in recorded maxima is such that this average is not significantly different from that of either the higher or lower sites ($P > 0.2$, Mann-Whitney U-test).

The absolute maximum shear force recorded by this apparatus with a sphere (2.99 N) agrees well with the maximum shear force recorded by the telemetry system with a replica limpet (2.80 N). The two objects are of similar size, have similar values for C_D and C_M (Table 4), and would thus be predicted to encounter similar forces by the theory outlined earlier (Eq. 3). These maximum shear forces are less than the estimated overall maximum force (4.68 N) because they do not include the lift force.

Predictability of maximum force direction—Only at the highest level on the shore (3.5 m above MLLW) was the direction of maximum wave force distinguishable from random over the sample of seven tides used in the comparison among heights (Table 3, G-test on the angular deviation: Zar 1974). In this case the average force came from a generally seaward direction (165° counterclockwise from seaward; 180° would represent a force coming directly from seaward). Over a longer series of measurements (44 tides) a significant direction of maximum force could be discerned at the site 2.75 m above MLLW. In that case the mean direction was 178° (angular deviation = 73.91°, $P < 0.01$).

Discussion

Exposure—Although it is interesting to know the magnitude and direction of the

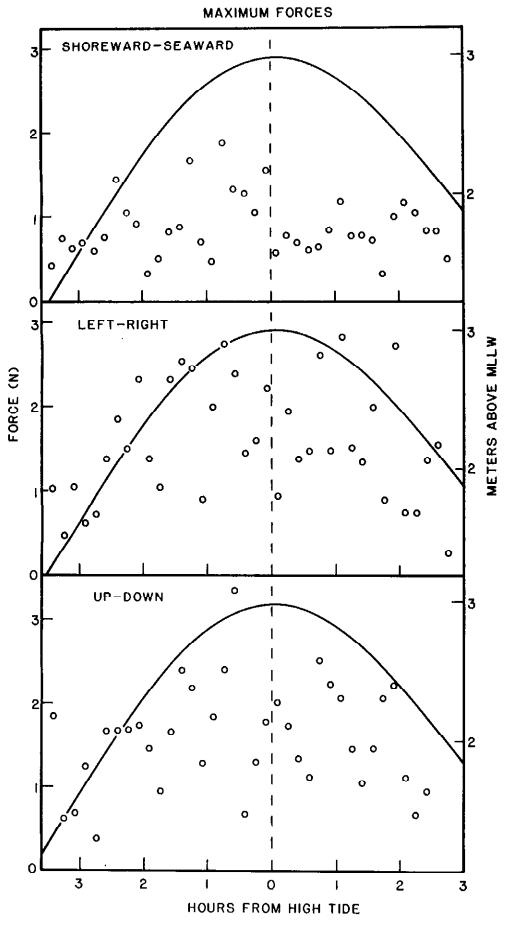

Fig. 10. Maximum force in each 10-min period as a function of time from high tide. The calculated still-water sea level is shown parenthetically (solid line) for visual correlation with the force values; this line is not a regression through the points plotted.

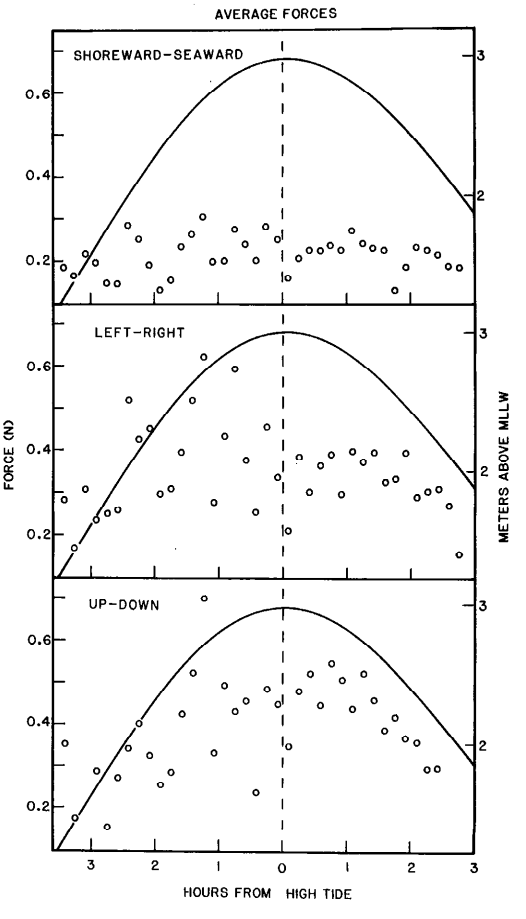

Fig. 11. As Fig. 10, but of average force.

forces exerted on a replica *C. pelta,* this information would be more valuable if compared to the ability of the organism to withstand such forces. The relative ability of the organism to withstand the forces imposed

Table 3. Data for maximum force over seven tides, simultaneous measurement at three emplacements. (N.S.—The mean angle is not significantly different from the arbitrarily chosen zero angle.)

H_s (m)	Mean max force (N)	SE	Mean angle	Angular deviation	P
1.65	0.864	0.193, $n = 8$	99.59°	74.85°	N.S.
2.75	1.149	0.332, $n = 12$	164.55°	95.54°	N.S.
3.50	0.767	0.171, $n = 10$	164.54°	51.95°	<0.01

Data for 44 tidal cycles (low tide to low tide) at the emplacement 2.75 m above MLLW
Absolute max force: 2.99 N
Avg max force: 1.57 N ($n = 30$, SD 0.805 N)
Avg angle: 178.25° counterclockwise from seaward ($n = 30$)
Angular deviation: 73.91° ($P < 0.01$)

Table 4. Force coefficients for various organisms and shapes, and the Re at which the C_D and C_L were measured. (N.A.—Not applicable.)

Object	C_D	C_L	C_M	Re
Limpets				
C. digitalis	0.52	0.25	1.84	10^5
C. pelta	0.45	0.47	1.68	10^5
Barnacle				
S. cariosus	0.52	N.A.	1.31	10^5
Snail				
T. canaliculata	0.67	—	1.72	10^5
Mussel				
M. californianus				
End-on	0.2*	—	1.2†	10^5
Broadside	0.8*	—	2.00†	10^5
Sphere	0.47‡	0.4	1.67§	10^5
Cylinder	0.73‡	N.A.	2.00§	10^5
Human	1.15‡	—	—	ca. 10^6

* Value for streamlined shape with thickness ⅓ the length; all other values from Denny et al. 1985.
† Daniel 1982.
‡ Hoerner 1965.
§ Sarpkaya and Isaacson 1981.

on it by waves can be used to define a quantifiable index of structural exposure.

$$\text{Structural exposure index, } \chi, = \frac{\text{Max wave force}}{\text{Max resistible force}}. \quad (9)$$

Both quantities that go into determining this index must be carefully defined and measured appropriately. For example, the maximum wave force depends on both the time over which forces are measured (Cartwright and Longuet-Higgins 1956) and the height distribution of the waves impinging on a site (itself a function of time). Further, the ability of an organism to resist a force can depend on the direction in which the force is applied and the rapidity with which the force is imposed (Grenon and Walker 1981).

The information presented here allows for a tentative first look at three aspects of the structural exposure index. First, exposure to normal forces. I use *C. pelta* as an example, this being the organism for which the most experimental data are available. For the purposes of this example I define the maximum force (Eq. 9) as the maximum normal force encountered during the sample tide (3.36 N), and the maximum resistible force as that required to dislodge an individual limpet in a direction normal to the substratum. For a limpet the size of the replica used, the foot area is about 4×10^{-4} m^3. Estimates of the average adhesive tenacity of stationary *C. pelta* when subjected to normal forces range from 6.8×10^4 N m^{-2} (Miller 1974) to 2.05×10^5 N m^{-2} (Denny et al. 1985). The resistible force, [tenacity (N m^{-2})] × [foot area (m^2)], is thus 27 or 82 N, depending on which tenacity value is used. The exposure index for normal forces, χ_N, thus lies in the range of 0.04–0.12 (Eq. 9).

The tensile tenacity of *C. pelta* decreases when the animal crawls. Miller (1974) measured a crawling tenacity of 2.5×10^4 N m^{-2}. Denny et al. (1985) noted a discrepancy between Miller's values measured on plastic substrata and those measured in the field. They estimated a crawling tenacity for *C. pelta* on rock substrata of 6.9×10^4 N m^{-2}. These values result in an exposure index about three times that for a stationary limpet (0.12–0.34). Further, these values for χ_N are calculated using the mean value for tenacity; limpets with less tenacity are at substantially higher risk of dislodgement.

Second, exposure to shear forces. The drag coefficients and adhesive tenacities in shear have been measured for several intertidal organisms (Table 4). The added mass coefficient has not been measured for organisms other than *C. pelta,* an acorn barnacle (*Semibalanus cariosus*), and a thaid snail (*Thais canaliculata*) (Denny et al. 1985). However, for the flow velocity and acceleration patterns measured in this study, the acceleration reaction contributes only about 10–15% of the total shear force exerted on the organism at the time of maximum force (Fig. 3, Eq. 2). Thus by calculating force based on drag alone we can calculate an exposure index for shear that is about 10–15% low.

The exposure index for shear can be calculated as a function of breaking wave height by using the relationship noted earlier (Eq. 1, 7) showing that to a first approximation drag is proportional to wave height. Thus Eq. 3 can be restated as

$$\text{Applied shear force} = 0.5\rho g(2.2H_B)SC_D, \quad (10)$$

and the exposure index for shear is

$$\chi_S = 0.5\rho g(2.2H_B)SC_D/\text{(shear tenacity} \times \text{foot area)}. \quad (11)$$

Values are plotted in Fig. 12 for waves up to $H_B = 10$ m, the maximum deep-water wave height observed near Tatoosh during the period 1946–1973 (U.S. Navy 1973). It is clear from this figure that different organisms exposed to the same flows are at widely varying risk of dislodgement due to shear forces.

These values for χ_S should be viewed with caution, however. Their calculation relies on the validity of the relationship between wave height at breaking and the velocity imposed on organisms (Eq. 6). Although the velocity information presented here supports this relationship, this information represents only one tide at one particular site; the similarity of predicted and observed values could be fortuitous. Further, the fact that higher waves break in deeper water (Eq. 8) means that the greater velocities associated with large waves may be attenuated before they reach a site on shore. At the site on Tatoosh Island the bottom slopes steeply, so that this effect is probably negligible. At sites with less steep bottom topography the effect may be substantial; Guza and Thornton (1982) discussed this topic.

Third, overall exposure. Because they do not take into account the interaction between normal and shear forces, the values of χ_N and χ_S calculated here underestimate the overall structural exposure index, χ. In a case where it was possible to estimate χ, the shear and normal tenacities of the limpet *C. digitalis* were the same (3.85×10^5 N m^{-2}) when measured on a rock substratum (Denny unpubl.). I assume that this same tenacity holds for forces applied simultaneously in both shear and normal directions. If we accept this assumption, a *C. digitalis* of the same size as the *C. pelta* considered previously can resist forces up to 15.4 N. The maximum vector force which (to a first estimate) could be encountered for the wave conditions present during the study period is 4.7 N (Table 1); thus χ for this stationary limpet could be as high as 0.31. The tenacity of *C. digitalis* when crawling is estimated by Denny et al. (1985) to decrease to 1.29×10^5 N m^{-2}, resulting in a χ of 0.91. These calculations are for the forces applied by waves maximally 4 m high at breaking. For storm waves 8 m high, the applied force can be expected to about double; in such circumstances χ could exceed 1 for a crawling *C. digitalis* with the mean tenacity and would be higher still for a limpet with less than average tenacity.

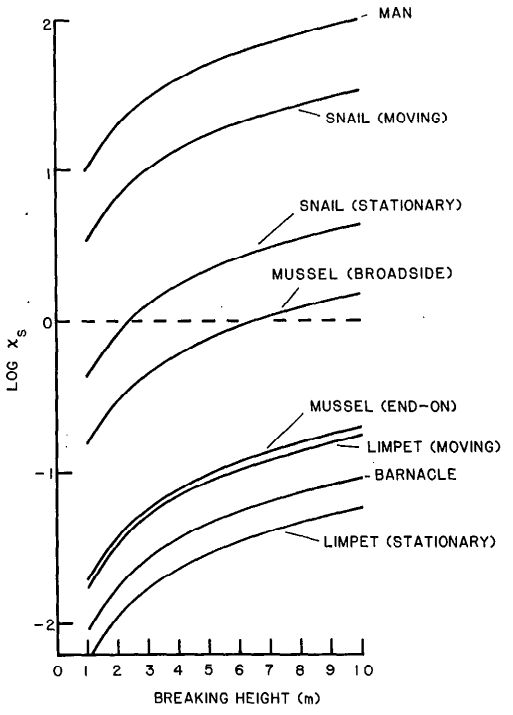

Fig. 12. Exposure index, χ_S, calculated for shear forces as a function of the height of breaking waves. The value of moving tenacity used in calculating χ_S for *C. pelta* is that of Denny et al. 1985. The value cited for a human being assumes that the wave impacts the person frontally, and that the person is capable of resisting a force of 1,110 N (150-lb force) applied at his midsection. The tremendous exposure index should give some tangibility to the forceful nature of the intertidal environment.

The structural exposure index proposed here provides information regarding only one aspect of the overall exposure of organisms. For instance, wave forces too small to dislodge a stationary limpet may be sufficient to cause a crawling limpet to stop (Wright 1978), and thereby may limit the animal's foraging time. However, because of the difficulties inherent in gathering data regarding the functioning of organisms in

wave-swept environments, quantitative information regarding the force limits to various functions does not yet exist and an examination of possible functional exposure indices is not possible here.

Predictability of force events—The data presented here suggest that the wave-swept environment due to a combination of sea and swell is unpredictable on the scale of seconds to hours. For example, consider a limpet which has just been subjected to a wave force of sufficient magnitude to cause it to stop crawling and adhere more tightly. Is there any way this limpet can predict how much time it has in which to forage again before the next large wave arrives? The power spectrum of this sample record (Fig. 8) suggests not. It is most probable that the next forceful wave will arrive in about 11 s, but this probability is not substantially higher than the probability that the next forceful wave will arrive before 11 s.

If the limpet can somehow gauge the height of the still-water level or the time from high tide, it could conceivably predict the frequency with which it will be immersed (Fig. 9), information potentially useful in avoiding desiccation. However, SWL (at least for the sample record) does not provide reliable information regarding the frequency with which waves causing potentially harmful forces arrive. The statistically significant correlations between force (both maximum and mean) and SWL or time probably do not account for enough of the variation in force to be biologically significant. This case clearly exemplifies the fact that predictability of the environment depends on the function in question.

Predictability of force as a function of height on the rock—The data presented here show that height on the rock was not a reliable indicator of maximum wave force over the course of seven tides because of the large variance about the mean maximum force, rather than the identity of the means themselves. This suggests that when information is available for a sufficiently large number of tides, the difference in means may become statistically (and biologically) significant.

It is possible to construct a model which qualitatively accounts for the observed means and allows for predictability of wave force as a function of height on the rock over long periods. Each wave hitting the shore on the Tatoosh site has the form shown schematically in Fig. 2. The central body of the wave can exert the maximal force of that wave and impacts the rock over a certain vertical distance, D. Areas of the rock above the initial impact zone are subjected to less-than-maximal velocities as the flow velocity decreases during run-up. At the base of the wave, the rising surge can interact with the backwash from the previous wave to form a protective cushion of water (Carstens 1968). Thus for each wave a limited section of the rock surface (that lying within vertical distance D of SWL) is subject to maximal forces. The location of this impact zone rises and falls with the tides. Depending on their height on the shore, H_S (Fig. 2), organisms at different heights spend a different amount of time in this zone during a tidal excursion. As the tide goes from low to high they enter the zone when SWL $= H_S - D$ and exit when SWL $= H_S$. By rearranging Eq. 7, we can calculate this time,

$$t = |(\tau/\pi)\cos^{-1}\{[2(H_S - L)/A] - 1\} - (\tau/\pi)\cos^{-1}\{[2(H_S - D - L)/A] - 1\}|. \quad (12)$$

The frequency, ω, with which waves break on shore is fairly regular. Thus each organism encounters a predictable number of waves, $N = \omega t$, during its residence in the zone of maximum force.

The force produced by each wave is, to a first approximation, a random selection from the exceedance distribution given by Fig. 4, and the probability that a certain wave imposes at least a certain force can thus be predicted.

If we assume these conditions, the probability of an organism at a certain level on the shore encountering a wave imposing a force corresponding to a certain frequency of occurrence can be calculated:

$$P = 1 - (1 - P_W)^N \quad (13)$$

where P_W is the probability of encountering a wave of at least a given force. The results of such a calculation are shown in Fig. 13. It has been assumed in this case that D is 1 or 2 m and that ves arrive every 10 s

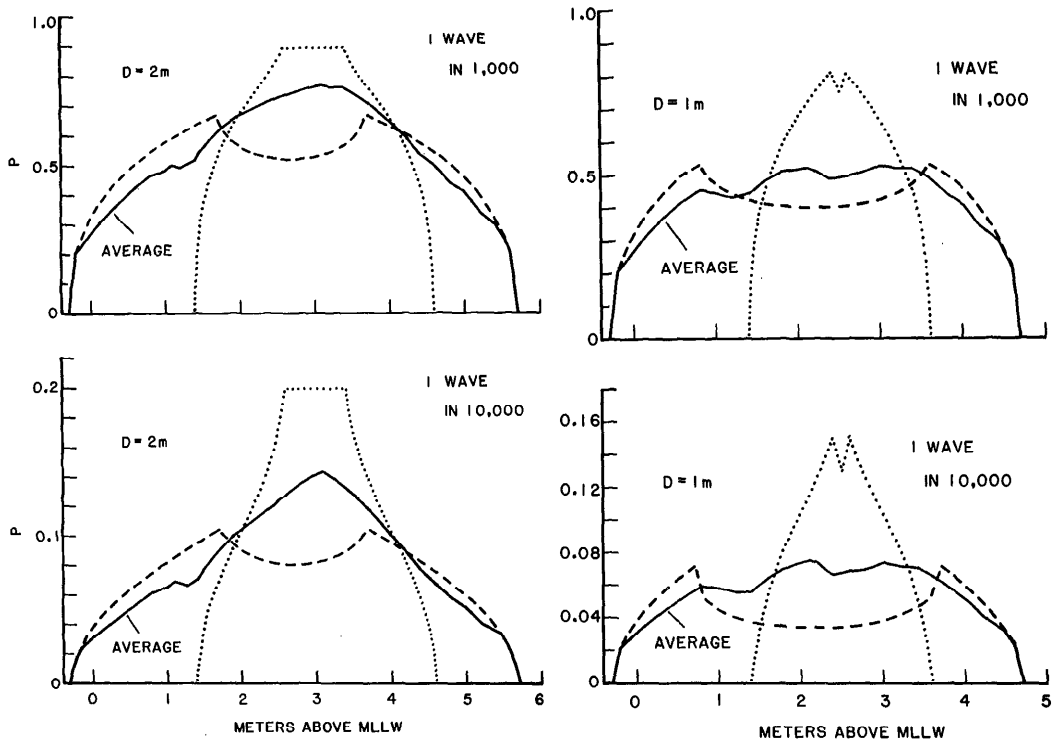

Fig. 13. The probability, P, of encountering a wave of a certain frequency of occurrence during one tidal excursion (low tide to high tide, or high tide to low tide). The height of the impact zone, D, is assumed to be 2 m (left) or 1 m (right). The dashed lines are for tidal excursions with $L = -0.3$ m, and $A = 4.0$ m. The dotted lines are for tidal excursions with $L = 1.4$ m, and $A = 1.2$ m. The solid lines are the average P for the 119 tidal excursions in January 1980. The upper graphs are calculated for a wave imposing a force of a magnitude seen on average only once in 1,000 waves; the lower graphs for 1 wave in 10,000.

($\omega = 360\ h^{-1}$). A monthly average tidal fluctuation for Tatoosh was used, based on information in the U.S. Dep. of Commerce tide tables for January 1980. Varying the magnitude of D quantitatively changes the H_S:probability curve, but does not qualitatively change the results.

This simple model predicts that the probability of encountering large hydrodynamic forces varies with height on the shore. For the values used here, the monthly average of P is highest near the H_S where the largest maximum force was measured (2.75 m above MLLW).

It is interesting that the height at which mussel beds are found (on Tatoosh, about 1.6–2.8 m above MLLW in exposed sites) corresponds roughly to the height range with the maximum average probability of encountering forceful flows. The tight packing of mussels in beds has often been suggested to be an ideal mechanism for coping with large wave forces (e.g. *see* Paine and Levin 1981; Ricketts et al. 1968). Each mussel protects its neighbors from encountering the mainstream water velocity; the bed as a whole essentially forms an unbroken new surface raised above the rock substratum. My model of force variation with height on the rock is so far speculative, but its correspondence with the available data is encouraging enough to warrant further investigation.

Consequences of the unpredictability of force direction—It has been shown above and elsewhere (e.g. Denny et al. 1985; Paine and Levin 1981) that wave forces can damage or dislodge a variety of intertidal organisms. However, most intertidal animals have drag coefficients that are quite high (*see Table 4*) compared to those of streamlined shapes where drag coefficients as low

as 0.05 are common (Hoerner 1965). Why have intertidal organisms not evolved more streamlined shapes? The answer lies partially in the unpredictability of flow direction in the intertidal zone. Vogel (1981) pointed out that streamlined shapes have low drag coefficients only when correctly oriented relative to flow. For example, a streamlined shape resembling a mussel may have a C_D for flow along its axis of 0.2, but a C_D of >0.8 when oriented broadside to the flow (Hoerner 1965). Thus, such a streamlined sessile organism, if caught in flows from the wrong direction, could encounter large drag forces, leading to high exposures (Fig. 12). As shown earlier, the flows in the intertidal zone are unpredictable in terms of direction over brief periods. Mussels generally avoid this problem by growing in densely packed beds.

Radially symmetrical organisms (e.g. cone-shaped limpets) present the same shape to flow from all directions and are therefore not subject to the problem described above. However, even these organisms may have a practical lower limit to their drag coefficient. A cone with a height-to-radius ratio of 0.5 has the low C_D of 0.30, but also has the high C_L of 0.46 (Denny unpubl.). This squat cone experiences a higher overall force than a more peaked cone (height:radius = 2, $C_D = 0.60$, $C_L = 0.27$: Denny unpubl.). The tradeoff between lift and drag may thus set limits to the proportions of radially symmetrical organisms. As noted earlier, the mechanism leading to lift requires the presence beneath the organism of a material that can transmit hydrostatic pressure. Organisms like bryozoans and coralline algae adhere to the substratum with solid glues and therefore are not subject to lift forces; many such organisms have encrusting forms where C_D approaches zero. It is less clear whether lift forces can act on sponges.

Impact pressures—Carstens (1968) pointed out that a wave breaking on the shore could exert very large impact pressures on the organisms present. Impact pressures as large as 1.5×10^7 N m^{-2} have been recorded (Carstens 1968), corresponding to a force of 6,000 N on the limpet replicas used here. These pressures occur when a mass of water moving normal to the surface of a rigid structure impacts the surface. The abrupt change in speed and direction brought about by impact results in a transient (2–5 ms) pressure (Wiegel 1964). Such pressures would appear to the telemetry apparatus used here as a very large transient force directed into the substratum at the very beginning of a wave-force event. In the 30 consecutive large waves that I examined in detail, the largest forces occurred at times considerably removed (>30 ms) from the initiation of force and are therefore clearly not impact forces. Of the nearly 1,000 wave-force events recorded on 19–20 November 1980, none showed a force large enough to be considered as due to wave impact.

This lack of wave impact forces is not surprising. The inclination of the substratum at the test site is such that the flows from breaking waves are seldom directed into the surface of the rock. Further, as Carstens (1968) noted, any compliance in the substratum or air entrained in the breaking wave substantially reduces the impact pressure. Collapsing waves such as those typical of the test site inevitably entrain air as they break; consequently the mass of water impacting the shore is compliant. The presence of surface irregularities and organisms on the substratum ensures that pockets of air are trapped at the substratum when water rushes over, increasing the substratum's compliance.

A final note—The conclusions drawn here regarding the nature of wave forces are based primarily on data from one tidal cycle at one very exposed site. I have no doubt that many of these conclusions are generally applicable to wave-swept sites, but until further evidence is available to support or refute them they should be regarded as tentative. For example, the information presented here pertains to waves comprised of both swell and locally generated seas. It seems likely that much of the unpredictability of the forces observed is due to the interaction of these two types of waves in randomly modulating the height of breakers. On days when only swell is present, wave force may be considerably more predictable. If this is true, it may be possible for organisms to sense (from the local wind speed, for instance) when the force envi-

ronment will be unpredictable and act accordingly. Further, the information here applies only to microhabitats fully exposed to mainstream flows. Organisms living in cracks and crevices, tide pools, and surge channels undoubtedly encounter different flows.

References

BATCHELOR, G. K. 1967. An introduction to fluid mechanics. Cambridge Univ.

CARSTENS, T. 1968. Wave forces on boundaries and submerged surfaces. Sarsia **34:** 37–60.

CARTWRIGHT, D. E., AND M. S. LONGUET-HIGGINS. 1956. The statistical distribution of the maxima of a random function. Proc. R. Soc. Lond. Ser. A **237:** 212–232.

CONNELL, J. H. 1972. Community interactions on marine rocky intertidal shores. Annu. Rev. Ecol. Syst. **3:** 169–192.

DANIEL, T. L. 1982. The role of added mass in locomotion with special reference to medusae. Ph.D. thesis, Duke Univ. 166 p.

———. 1984. Unsteady aspects of aquatic locomotion. Am. Zool. **24:** 121–134.

DENNY, M. W. 1982. Forces on intertidal organisms due to breaking ocean waves: Design and application of a telemetry system. Limnol. Oceanogr. **27:** 178–183.

———. 1983. A simple device for recording the maximum force exerted on intertidal organisms. Limnol. Oceanogr. **28:** 1269–1274.

———, T. L. DANIEL, AND M. A. KOEHL. 1985. Mechanical limits to size in wave-swept organisms. Ecol. Monogr. **55:** 69–102.

GALVIN, C. J. 1972. Waves breaking in shallow water, p. 413–456. *In* R. E. Meyer [ed.], Waves on beaches and resulting sediment transport. Academic.

GRENON, J.-F., AND G. WALKER. 1981. The tenacity of the limpet *Patella vulgata* L.: An experimental approach. J. Exp. Mar. Biol. Ecol. **54:** 277–308.

GUZA, R. T., AND A. J. BOWEN. 1976. Resonant interactions for waves breaking on a beach, p. 560–579. *In* Conf. Coastal Eng. Proc. 1976. Am. Soc. Civ. Eng.

———, AND E. B. THORNTON. 1982. Swash oscillations on a natural beach. J. Geophys. Res. **87:** 483–491.

HARGER, J. R. 1970. The effects of wave impact on some aspects of the biology of sea mussels. Veliger **12:** 401–414.

HOERNER, S. F. 1965. Fluid-dynamic drag. Hoerner.

JENKINS, G. M., AND D. G. WATTS. 1968. Spectral analysis and its application. Holden-Day.

JONES, W. E., AND A. DEMETROPOULOS. 1968. Exposure to wave action: Measurements of an important ecological parameter on the shores of Anglesey. J. Exp. Mar. Biol. Ecol. **2:** 46–63.

KOEHL, M. A. 1977. Effects of sea anemones on the flow forces they encounter. J. Exp. Biol. **69:** 87–105.

———. 1982. The interaction of moving water and sessile organisms. Sci. Am. **247:** 124–134.

———. 1984. How benthic organisms withstand moving water. Am. Zool. **24:** 57–69.

LEWIS, J. P. 1968. Water movements and their role in rocky shore ecology. Sarsia **34:** 13–36.

LONGUET-HIGGINS, M. S. 1952. On the statistical distribution of the heights of sea waves. J. Mar. Res. **11:** 245–266.

LUBCHENCO, J., AND B. A. MENGE. 1978. Community development and persistence in a low rocky intertidal zone. Ecol. Monogr. **48:** 67–94.

MENGE, B. A. 1972. Foraging strategy of a starfish in relation to actual prey availability and environmental predictability. Ecol. Monogr. **42:** 25–50.

———. 1978. Predation intensity in a rocky intertidal community. Oecologia **34:** 1–16.

MILLER, S. L. 1974. Adaptive design of locomotion and foot form in prosobranch gastropods. J. Exp. Mar. Biol. Ecol. **14:** 99–156.

NEWELL, R. C. 1979. Biology of intertidal animals, 3rd ed. Mar. Ecol. Surv.

NOWELL, A. R., AND P. A. JUMARS. 1984. Flow environments of aquatic benthos. Annu. Rev. Syst. Ecol. **15:** 303–328.

PAINE, R. T., AND S. A. LEVIN. 1981. Intertidal landscapes: Disturbance and the dynamics of pattern. Ecol. Monogr. **51:** 145–178.

QUINN, J. F. 1979. Disturbance, predation and diversity in the rocky intertidal zone. Ph.D. thesis, Univ. Washington. 225 p.

RICKETTS, E., J. CALVIN, AND J. W. HEDGPETH. 1968. Between Pacific tides, 4th ed. Stanford.

SARPKAYA, T., AND M. ISAACSON. 1981. Mechanics of wave forces on offshore structures. Van Nostrand-Reinhold.

SOUSA, W. P. 1984. The role of disturbance in natural communities. Annu. Rev. Syst. Ecol. **15:** 353–391.

THORNTON, E. B., AND R. T. GUZA. 1983. Transformation of wave height distribution. J. Geophys. Res. **88:** 5925–5938.

U.S. ARMY CORPS OF ENGINEERS. 1977. Shore protection manual. V. 1. U.S. GPO.

U.S. NAVY. 1973. Summary of synoptic meteorological observations. Natl. Tech. Inform. Serv.

VOGEL, S. 1981. Life in moving fluids. Grant.

WIEGEL, R. L. 1964. Oceanographical engineering. Prentice-Hall.

WRIGHT, W. G. 1978. Aspects of the ecology and behavior of the owl limpet, *Lottia gigantea,* Sowerby, 1834. West. Soc. Malac. Annu. Rep. 11, p. 7.

ZAR, G. H. 1974. Biostatistical analysis. Prentice-Hall.

Submitted: 16 July 1984
Accepted: 6 May 1985